Raman Study of the Polarizing Forces Promoting Catalysis in 4-Chlorobenzoate-CoA Dehalogenase†

John Clarkson,‡ Peter J. Tonge,§ Kim L. Taylor,|| Debra Dunaway-Mariano,|| and Paul R. Carey*,‡

Department of Biochemistry, Case Western Reserve University, 10900 Euclid Avenue, Cleveland, Ohio 44106, Department of Chemistry, State University of New York at Stony Brook, Stony Brook, New York 11794, and Department of Chemistry and Biochemistry, University of Maryland, College Park, Maryland 21742

Received April 23, 1997; Revised Manuscript Received June 12, 1997⊗

ABSTRACT: The enzyme 4-chlorobenzoate-CoA dehalogenase catalyzes the hydrolysis of 4-chlorobenzoate-CoA (4-CBA-CoA) to 4-hydroxybenzoyl-CoA (4-HBA-CoA). In order to facilitate electrophilic catalysis, the dehalogenase utilizes a strong polarizing interaction between the active site residues and the benzoyl portion of the substrate [Taylor, K. L., *et al.* (1995) *Biochemistry 34*, 13881]. As a result of this interaction, the normal modes of the benzoyl moiety of the bound 4-HBA-CoA undergo a drastic rearrangement as shown by Raman spectroscopy. Here, we present Raman difference spectroscopic data on the product−enzyme complex where the product's benzoyl carbonyl is labeled with ^{18}O (C═^{18}O) or ^{13}C (^{13}C═O) or where the 4-OH group is labeled with ^{18}O. The data demonstrate that the carbonyl group participates in the most intense normal modes occurring in the Raman spectrum in the 1520−1560 cm^{-1} region. The substrate analog 4-methylbenzoate-CoA (4-MeBA-CoA) has also been characterized by Raman difference spectroscopy in its free form and bound to the dehalogenase. Upon binding, the 4-MeBA-CoA shows evidence of polarization within the delocalized π-electrons, but to a lesser extent compared to that seen for the product. The use of 4-MeBA-CoA labeled with ^{18}O at the carbonyl enables us to estimate the degree of electron polarization within the C═O group of the bound 4-MeBA-CoA. The C═O stretching frequency occurs near 1663 cm^{-1} in non-hydrogen bonding solvents such as CCl_4, near 1650 cm^{-1} in aqueous solution, and near 1610 cm^{-1} in the active site of dehalogenase. From model studies, we can estimate that in the active site the carbonyl group behaves as though it is being polarized by hydrogen bonds approximately 57 kJ mol^{-1} in strength. Major contributions to this polarization come from hydrogen bonds from the peptide NHs of Gly114 and Phe64. However, an additional contribution, which may account for up to half of the observed shift in $\nu_{C=O}$, originates in the electrostatic field due to the α-helix dipole from residues 121−114. The helix which terminates at Gly114, near the C═O group of the bound benzoyl, provides a dipolar electrostatic component which contributes to the polarization of the C═O bond and to the polarization of the entire benzoyl moiety. The effect of both the helix dipole and the hydrogen bonds on the C═O is a "pull" of electrons onto the carbonyl oxygen, which, in turn, polarizes the electron distribution within the benzoyl π-electron system. The ability of these two factors to polarize the electrons within the benzoyl moiety is increased by the environment about the benzoyl ring; it is surrounded by hydrophobic residues which provide a low-dielectric constant microenvironment. Electron polarization promotes catalysis by reducing electron density at the C4 position of the benzoyl ring, thereby assisting attack by the side chain of Asp145. An FTIR study on the model compound 4-methylbenzoyl *S*-ethyl thioester, binding to a number of hydrogen bonding donors in CCl_4, is described and is used to relate the observed shift of the C═O stretching mode of 4-MeBA-CoA in the active site to the hydrogen bonding strength value. Since the shift of the C═O frequency upon binding is due to hydrogen bonding and helix dipole effects, we refer to this bonding strength as the effective hydrogen bonding strength.

4-Chlorobenzoate-coenzyme A dehalogenase catalyzes the hydrolytic dehalogenation of 4-chlorobenzoate-coenzyme A (4-CBA-CoA) to 4-hydroxybenzoate-CoA (4-HBA-CoA). This enzyme has been discovered in a number of soil-dwelling bacterial strains where it functions along with 4-CBA-CoA ligase and 4-HBA-CoA thioesterase to convert *p*-chlorobenzoic acid to *p*-hydroxybenzoic acid (for a review, see ref 1). Studies of the *Pseudomous* sp. strain CBS3 4-CBA-CoA dehalogenase have shown that it utilizes a unique form of catalysis in which an active site carboxylate bonds to C4 of the benzoyl ring of the bound substrate to form a Meisenheimer complex which then proceeds to product through chloride ion expulsion, the formation of an arylated intermediate, and hydrolysis as seen in Scheme 1 (*2*, *3*).

The nature of the active site forces which increase the electrophilic character of the C4 position is of interest since the formation of a Meisenheimer-like complex in the reaction is not chemically facile (*4*, *5*). An indication that strong electrostatic forces are present in the active site came from

† This work was supported by NIH Grants GM-36360 (to D.D.-M.) and GM-54072 (to P.R.C.).

* Author to whom correspondence should be addressed. E-mail: carey@biochemistry.cwru.edu. Fax: (216) 368-4544.

‡ Case Western Reserve University.

§ State University of New York at Stony Brook.

|| University of Maryland.

⊗ Abstract published in *Advance ACS Abstracts,* August 1, 1997.

S0006-2960(97)00941-0 CCC: $14.00

Scheme 1: Proposed Chemical Pathway for the Hydrolysis of 4-CBA-CoA by Dehalogenase (*8*)

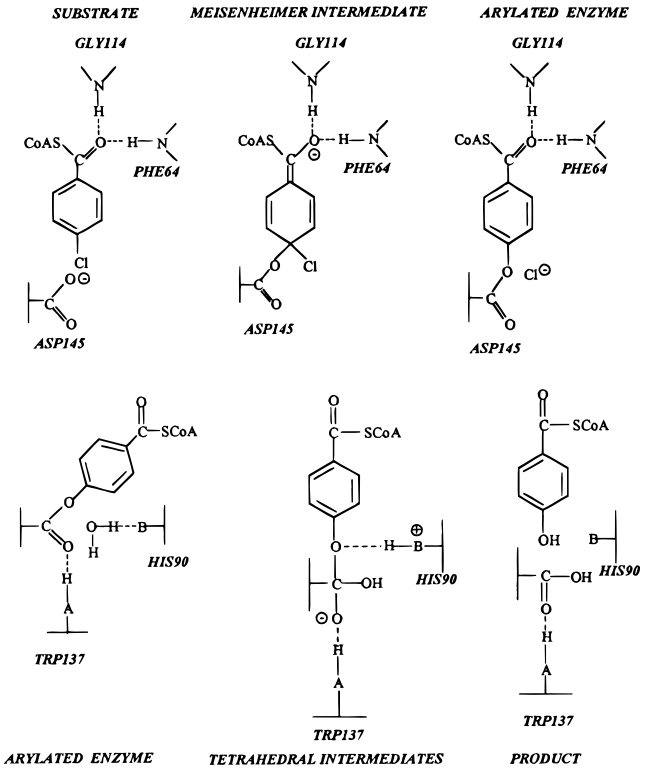

absorption, Raman, and NMR spectroscopic studies of enzyme complexes involving the product and, separately, a substrate analog (*6*). The spectroscopic data showed that electron-polarizing forces can be brought to bear in the active site, which, in the case of the bound product, cause a major rearrangement of the electrons in the benzoyl moiety. Interest in these findings has recently been heightened by the publication of the structure of the dehalogenase−4-HBA-CoA complex derived by X-ray crystallography (*7*), and the X-ray results have been used to analyze shifts in absorption maxima for ligand−enzyme complexes involving several site-selected mutants (*8*). Thus, we now have access to both structural and spectroscopic data on a complex which exhibits strong polarization, and we have the opportunity of relating the observed spectroscopic effects to structural determinants. In particular, an α-helix, with its attendant dipole effects, appears to play a key role in polarizing the substrate's electrons, and we can discuss this interaction in structural terms.

The roles of α-helix dipoles in stabilizing charged groups in proteins (*9*) and in modulating side chain pK_as (*10*, *11*) are well-recognized, with recent consensus favoring the importance of local dipoles (*9*), rather than a macrodipole, in generating an electrostatic field. It is also recognized that the field can bring about a red shift in the absorption spectrum of a chromophoric group bound near the α-helix's N terminus (*12*, *13*). In addition, it has been suggested that α-helix dipoles can contribute to catalytic rate enhancement (*14*), and recent Raman and absorption spectroscopic studies on a series of acyl cysteine proteases (*15*, *16*) have provided quantitative support for this notion. When chromophoric acyl groups bind to cysteine proteases, substantial red shifts, of up to 60 nm, occur, which can be accompanied by major changes in the acyl group's Raman spectrum (*12*). An α-helix, which terminates at the active site cysteine, has been proposed as the source of observed spectroscopic effects, with the α-helix dipole causing polarization of the acyl group's π-electrons. Although extensive spectroscopic and kinetic data have been reported for the acyl cysteine proteases, and it has been possible to suggest that the α-helix dipole promotes catalysis by helping stabilize charge buildup in the transition state, hard structural data on how the α-helix interacts with the chromophore are lacking. Thus, the structure of the 4-HBA-CoA dehalogenase provides the first opportunity to characterize a structure involving an α-helix−chromophore interaction which brings about polarization of the chromophore's electrons.

In the spectroscopic aspects of the present work, we have used $^{13}C{=}O$, $C{=}^{18}O$, and 4-^{18}OH isotopomers of 4-HBA-CoA to gauge the degree of participation of the benzoyl C═O and 4-OH groups in the intense Raman modes seen for the bound product. We have also studied the substrate analog 4-MeBA-CoA and its $C{=}^{18}O$ isotopomer to gain an estimate of the degree of shift in the C═O stretching frequency upon binding in the active site. At the same time, we have undertaken extensive analysis of hydrogen bonding to the model compound 4-methylbenzoate *S*-ethyl thioester which enables us to form a semiquantitative estimate of the strength of the forces acting on the 4-MeBA-CoA's thioester carbonyl in the active site.

EXPERIMENTAL PROCEDURES

Materials

4-CBA-CoA dehalogenase was purified from *Escherichia coli* K38 cells according to the procedure of Chang *et al.* (*17*) as modified by Liang *et al.* (*18*). 4-HBA-CoA and 4-MeBA-CoA were prepared in the manner described previously (*6*, *18*).

The model compound, 4-methylbenzoyl *S*-ethyl thioester, was synthesized using the protocol described for 4-hydroxybenzoyl thiolester (*6*).

Isotopically Labeled Compounds. 4-[$^{13}C{=}O$]hydroxybenzoic acid was purchased from Isotec Inc.

4-[Thioester-$^{13}C{=}O$]HBA-CoA. This compound was synthesized from 4-[$^{13}C{=}O$]hydroxybenzoic acid by using the basic procedure reported by Merkel *et al.* (*19*) which was further adapted and reported by Liang *et al.* (*18*).

4-[^{18}O]HBA-CoA. Solid 4-CBA-CoA (10 mg) was dissolved in 1 mL of $H_2{}^{18}O$ (99.2%) and converted to 4-HBA-CoA by the addition of 31 μL of 4-CBA-CoA dehalogenase (in buffered $H_2{}^{16}O$, 3.7 mg/mL; specific activity = 1.5 units/mg) to give 11.4 mM 4-CBA-CoA and 10 μM 4-CBA-CoA dehalogenase in 5 mM K^+Hepes (pH 7.0) (96% $H_2{}^{18}O$). After 6 h at 25 °C, the 4-[^{18}O]HBA-CoA was purified by gel filtration chromatography (Sephadex G-25 column, 110 × 2.2 cm) using H_2O as an eluant. Fractions containing pure compound were collected and lyophilized to dryness. Two hundred micrograms was dissolved in 100 mL of 5 mM K^+-Hepes (pH 7.0) ($H_2{}^{16}O$) containing 11 units of 4-HBA-CoA thioesterase. Following 15 min of incubation at 25 °C, the protein was removed from the solution using a Centricon-10 concentrator. The 4-HBA-containing solution was then acidified with 1 N HCl to pH 1 and extracted four times with 1 mL portions of ethyl acetate. The ethyl acetate extracts were combined and dried over anhydrous sodium sulfate and then concentrated to a solid *in vacuo*. The solid

was dissolved in 0.5 mL of absolute methanol and added to 2.5 mL of anhydrous ethyl ether in a MNNG (1-methyl-3-nitro-1-nitrosoguanidine) diazomethane generator. The methylation reaction was initiated by the addition of 0.6 mL of 5 N sodium hydroxide to 133 mg of the MNNG precursor. After approximately 15 h at 25 °C, the methanol/ether solution (which had evaporated to approximately 0.5 mL) was subjected to analysis by GC−MS. The methyl 4-methoxybenzoate product was identified by comparison with the authentic compound. GC−MS (MeOH/Et_2O): t_R = 7.48 min, *m*/*e* (amu) 166/168/170 (M*), 135/137/139 (M* − OCH_3), 107/109 (M* − $COOCH_3$), 92/92 (M* − $COOCH_3$-OCH_3). The 4-HBA-CoA was found to have 89% ^{18}O in the hydroxyl position by GC−MS analysis.

4-[thioester-^{18}O═C]HBA-CoA. Hepes (23.8 mg), 3.14 mg of 4-CBA, 15.4 mg of CoA, 55.1 mg of ATP (disodium salt), and 3 mg of $MgCl_2 \cdot 6H_2O$ were dissolved in 3 mL of $H_2{}^{18}O$ (99.2%), and the pH was raised to 7.5 with the slow addition of 38 mL of 10 M KOH, yielding approximately 50 mM K^+Hepes (pH 7.5), 6.7 mM 4-CBA, 6.7 mM CoA, 33.5 mM ATP and 5 mM $MgCl_2$. Five units of inorganic pyrophosphatase, 1 unit of 4-CBA:CoA ligase, and 10 units of 4-HBA-CoA thioesterase were added to yield a final volume of 3.1 mL (96% $H_2{}^{18}O$). After 4 h, 55.1 mg of ATP was added and the pH of the resulting solution was adjusted to 7.5 with 10 M KOH. 4-CBA:CoA ligase (1.5 units), 15 units of 4-HBA-CoA thioesterase, and 5 units of inorganic pyrophosphatase were added, and the reaction mixture was incubated at 25 °C overnight. The enzymes were then removed by centrifugation of the solution through a Centricon-10 concentrator (2 h at 5000 rpm). Unreacted 4-CBA was converted to 4-CBA-CoA by incubating the solution with 1.4 units of 4-CBA:CoA ligase and 5 units of inorganic pyrophosphatase. The enzymes were removed by precipitation by vortexing the solution with 2 mL of CCl_4. The aqueous layer was dried *in vacuo*. The residue was dissolved in 5 mL of $H_2{}^{16}O$, and the pH of the resulting solution was adjusted to 7.5 with 10 M KOH. Two units of 4-CBA-CoA dehalogenase was added, and after 4 h, the enzyme was precipitated by vortexing the solution with 2 mL of CCl_4. The ^{18}O-labeled 4-HBA-CoA was purified by preparative, reversed-phase HPLC using a Beckman Gold system, 110B pumps, and a Whatman ODS-3 column. Solvent A was 50 mM sodium acetate at pH 5.0, and solvent B was acetonitrile. A linear gradient was run from 10 to 25% solvent B in 10 min, followed by a linear gradient of 25 to 75% in 10 min. The flow was 20 mL/min, and the absorbance of the effluent was monitored at 260 nm. The peak containing 4-HBA-CoA (retention time = 8.0 min) was collected and desalted using preparative, reversed-phase HPLC with 1% methanol in water for 10 min, followed by a linear gradient of 1 to 50% methanol in water for 10 min at a flow rate 20 mL/min. The single major peak (retention time = 5.5 min) was collected and lyophilized to give 6.7 mg of 4-[*thioester*-^{18}O═C]HBA-CoA (34%, 7.0 μmol).

In order to determine the percentage of ^{18}O in the carbonyl oxygen, the compound was converted to 4-HBA-CoA thioesterase and the product was derivatized and analyzed by GC−MS according to ref 2 as described above. GC−MS (MeOH/Et_2O): t_R = 6.08 min, *m*/*e* (amu) 166/168/170 (M*), 135/137/139 (M* − OCH_3), 107/109 (M* − $COOCH_3$), 92/92 (M* − $COOCH_3OCH_3$). The product was found to contain 75% ^{18}O in the thioester carbonyl oxygen.

4-[thioester-^{18}O═CMeBA-CoA. Three milliliters of 50 mM K^+Hepes (pH 7.5) containing 5 mM $MgCl_2$ and 12.0 mM 4-MeBA-CoA was lyophilized to dryness and was reconstituted in 3 mL of $H_2{}^{18}O$ (99.2% ^{18}O-enriched). To the solution were added 3.14 mg of 4-CBA, 15.4 mg of CoA, and 55.1 mg of ATP (disodium salt). The pH of the resulting mixture was raised to pH 7.5 by the slow addition of 38 μL of 10 M KOH (in $H_2{}^{16}O$), yielding approximately 50 mM K^+Hepes (pH 7.5), 12.0 mM 4-MeBA-CoA, 6.7 mM CoA, 33.5 mM ATP, and 5 mM $MgCl_2$. Five units of inorganic pyrophosphatase, 1 unit of 4-CBA:CoA ligase, and 30 units of 4-HBA-CoA thioesterase were added to yield a final volume of 3.2 mL (94.3% $H_2{}^{18}O$). After 4 h, 55.1 mg of ATP was added and the pH was adjusted to 7.5 with 10 M KOH. One unit of 4-CBA:CoA ligase, 30 units of 4-HBA-CoA thioesterase, and 5 units of inorganic pyrophosphatase were added, and the reaction was allowed to run overnight at 25 °C. The enzymes were then removed by centrifugation of the solution in a Centricon-10 concentrator (2 h at 5000 rpm). The remaining 4-MeBA was converted to 4-MeBA-CoA by incubating the solution in the presence of a freshly added mixture of 55.1 mg of ATP, 15.4 mg of CoA, 5 mM $MgCl_2$, 2 units of 4-CBA:CoA ligase, and 5 units of inorganic pyrophosphatase. The enzymes were removed by vortexing the solution with 2 mL of CCl_4 to precipitate the enzyme, and the aqueous layer was dried. The 4-[*thioester*-^{18}O═C]-MeBA-CoA was purified by preparative, reversed-phase HPLC (Whatman ODS-3 column). Solvent A was 50 mM sodium acetate at pH 5.0, and solvent B was acetonitrile. A linear gradient was run from 10 to 25% solvent B in 10 min, followed by a linear gradient of 25 to 75% solvent B in 10 min. The flow rate was 20 mL/min, and the absorbance of the effluent was monitored at 260 nm. The peak containing 4-HBA-CoA (retention time = 15.6) was collected and concentrated. The compound was desalted using preparative, reversed-phase HPLC with 1% methanol in water for 3 min, followed by a linear gradient of 1 to 90% methanol in water for 10 min, followed by 2 min in 95% methanol at a flow rate of 20 mL/min. The single major peak (retention time = 13.6 min) was collected and lyophilized to give solid 4-[*thioester*-^{18}O═C]MeBA-CoA.

In order to determine the percentage of ^{18}O in the carbonyl oxygen, the compound was converted to 4-MeBA by 4-HBA-CoA thioesterase and was analyzed for ^{18}O enrichment by GC−MS. The 4-[*thioester*-^{18}O═C]MBA product was identified by comparison with the authentic compound 4-methylbenzoate. GC−MS (MeOH/Et_2O) t_R = 9.93 min, *m*/*e* (amu) 136/138 (M*). The product was found to contain 78% ^{18}O in the thioester carbonyl oxygen.

Raman Spectral Measurements

Raman spectra were acquired from a Spex 0.5 m single monochromator equipped with a CCD detector and a supernotch filter (*20*). Five hundred milliwatts of 647.1 nm radiation from a krypton ion laser were used to obtain the spectra, using 90° scattering geometry. Samples were contained in a 50 μL quartz cuvette and were buffered with 50 mM Hepes (pH 7.5) at ambient temperature. The concentrations of ligand and enzyme used are provided in the figure legends, along with the exposure time. The Raman difference technique used to record the spectrum of unbound

ligand in buffer and ligand bound to enzyme has been described previously (*6*).

FTIR Model Studies

The relationship between the shift in the carbonyl stretching frequency and the enthalpy of hydrogen bond formation for the model compound 4-methylbenzoate *S*-ethyl thioester was determined by FTIR in a manner similar to that outlined by Tonge *et al.* (*21*) for α,*β*-unsaturated esters. In three series of experiments, hydrogen bonding of the model compound's C═O to the hydrogen bonding donors, ethanol (pK_a = 15.5), phenol (pK_a = 9.99), and 3,5-dichlorophenol (pK_a = 8.18), was studied in CCl_4 as a function of temperature.

The concentration of the donor was kept constant at 6 mM for ethanol and 3 mM for phenol and 3,5-dichlorophenol, to avoid self-association. The concentration of the model compound, 4-methylbenzoate *S*-ethyl thioester, was varied in the range of 0−50 mM in 10 mM steps. FTIR spectra were obtained with a Bomem MB-Series spectrometer, with a 0.5 mm path length KBr sample cell. The temperature of the cell was controlled with cryosolvent (30% ethylene glycol) circulating through the cell holder and was monitored using a thermocouple inserted into a hole drilled into the side of one of the KBr windows.

For each donor−acceptor pair, a temperature range of 174−317 K was used.

From the integrated area of the FTIR ν_{O-H} peak (ν_{O-H} free, ethanol, 3632 and 3626 cm^{-1}; phenol, 3609 cm^{-1}; and 3,5-dichlorophenol, 3599 cm^{-1}), the concentration of free donor ([donor]$_{free}$) can be found for each concentration of model compound used. Using [donor]$_{free}$, both [donor]$_{bound}$ and [model compound]$_{free}$ were calculated, and *K*, the equilibrium constant for hydrogen bond formation, was calculated by plotting [donor]$_{bound}$ against [model compound-]$_{free}$ × [donor]$_{free}$ [(K = [donor]$_{bound}$/[model compound]$_{free}$ × [donor]$_{free}$)]. *K* was determined for every temperature and −Δ*H* obtained using the van't Hoff equation ($\ln K = -\Delta H/RT + \Delta S/R$) by plotting ln *K* vs 1/*T*.

$\Delta\nu_{C=O}$, the decrease in the carbonyl frequency of the model compound upon hydrogen bond formation with a donor, was determined by adding an excess of donor (0.1 M) to 20 mM model compound and by curve fitting the carbonyl region to find the new hydrogen-bonded carbonyl frequency. Alternatively, an FTIR spectrum of free acceptor was interactively subtracted from that of a solution containing excess donor and acceptor to confirm that the values for the hydrogen-bonded carbonyl frequency were for the C═O bound to a single donor molecule. Curve fitting was performed with Spectracalc (Galactic Industries).

RESULTS AND DISCUSSION

Using Isotopic Substitution To Gain Insight into the Raman Modes of Bound 4-HBA-CoA. 4-HBA-CoA in buffer, near neutral pH, gives rise to Raman peaks at 1646 cm^{-1} due to the carbonyl stretch of the thioester, phenyl ring modes (8a and 8b) at 1603 and 1589 cm^{-1} , and in-plane phenyl hydrogen bending modes at 1221 and 1173 cm^{-1} (*6*). As we have shown (*6*), binding to dehalogenase results in a profound change in the Raman spectrum of 4-HBA-CoA. In essence, all the major features mentioned above "disappear", and the difference spectrum of the bound 4-HBA-CoA is dominated by three features at 1560, 1537, and 1524 cm^{-1} shown in Figure 1 (the 1537 cm^{-1} feature can be resolved by "curve fitting" this region of the spectrum). In order to gain insight into the large changes observed in the Raman spectrum, three isotopomers of 4-HBA-CoA are now examined; these have ^{18}O at the 4-hydroxylbenzoyl position (^{18}O−H) ^{18}O at the thioester carbonyl (C═^{18}O), or ^{13}C at the thioester carbonyl (^{13}C═O). The results are striking in that they indicate that the intense Raman modes seen for the bound product in Figure 1, between 1525 and 1560 cm^{-1}, all contain a contribution from motions of the thiolester C═O group.

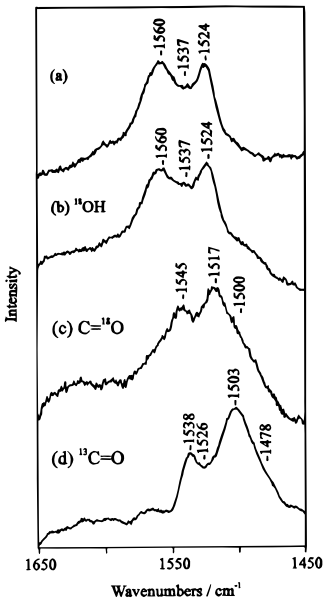

FIGURE 1: Raman difference spectra, in the range of 1450−1650 cm^{-1}, of (a) unlabeled 1 mM 4-HBA-CoA bound to 1 mM dehalogenase, (b) 1 mM ^{18}OH-labeled 4-HBA-CoA bound to 1 mM dehalogenase, (c) 1 mM C═^{18}O-labeled 4-HBA-CoA bound to 1 mM dehalogenase, and (d) 1 mM ^{13}C═O-labeled 4-HBA-CoA bound to 1 mM dehalogenase. Solutions were buffered in 50 mM Hepes at pH 7.5. The spectroscopic conditions were 647.1 nm Kr laser excitation, 750 mW, and 40 accumulations of 10 s each.

Table 1: Peak Positions for the Most Intense Features in the Raman Spectra of 4-HBA-CoA in Its *p*-OH and -O$^-$ Forms[a]

	C═O	8a, 8b	C−H bends (phenyl) (cm^{-1})
	Neutral pH OH Form		
unlabeled	1646	1603, 1589	1221, 1173
p-^{18}OH	1645	1602, 1587	1220, 1172
^{13}C═O	1605 (sh)	1592, 1579	1213, 1170
C═^{18}O	1608 (sh)	1599, 1583	1220, 1172
	pH 10 O$^-$ Form		
unlabeled	1628	1576	1235, 1161
p-^{18}O$^-$	1631	1578	1226, 1160
^{13}C═O	nd	1570	1221, 1160
C═^{18}O	nd	1574	1228, 1161

[a] nd = not detected. sh = shoulder. 8a and 8b are a degenerate pair of C−C stretching modes associated with the phenyl ring (*27*).

For the free isotopomers in aqueous solution, the positions of the major Raman features are summarized in Table 1. The results in Table 1 demonstrate that, for the free product molecule in its OH form, the *p*-hydroxy group oxygen makes no significant contribution to the main normal modes seen in the Raman spectrum, the C═O oxygen atom makes a small contribution (see the small down shift of the 8a and

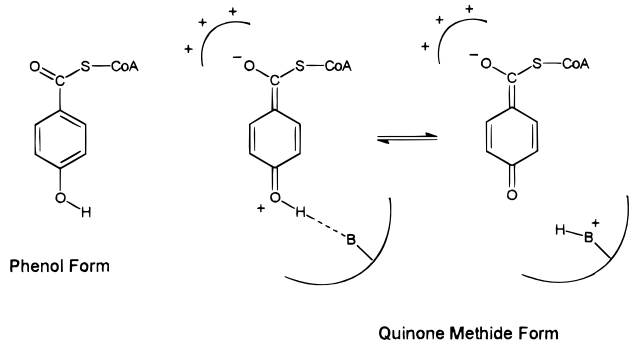

FIGURE 2: Phenol form of 4-HBA-CoA which is dominant in buffer solution and the quinone methide form of 4-HBA-CoA bound to dehalogenase. B is an active site base.

8b modes), and the C═O carbon makes a modest contribution as shown by the ~10 cm^{-1} downshifts of the 8a and 8b modes upon ^{13}C═O substitution. For the ionized O^- form, apart from the apparent diminution of the intensity for the C═O stretch upon substitutions of ^{13}C or ^{18}O into this linkage, neither the *p*-O^- atom nor the -C═O group appears to be coupled into the observed normal modes.

The contrast of the isotopomer results for the free ligand with those for the bound, set out in Figure 1, is quite striking. Figure 1 shows that the Raman profile for the bound product, which contains peaks at 1561, 1537, and 1524 cm^{-1} , is unaffected by ^{18}OH substitution and thus the *para* substituent plays little role in the observed normal modes. However, substitution in the carbonyl brings about large changes in the profile with the most marked effect being observed for ^{13}C═O substitution (Figure 1). These results provide compelling evidence that, for the bound product molecule, the C═O group is strongly vibrationally coupled into the intense Raman modes observed in the 1520−1560 cm^{-1} region.

A comparison of the Raman results for the free and bound product allows us to draw several conclusions. Upon binding, a major rearrangement of the benzoyl group's π-electrons occurs. Since Raman peak positions are a property solely of the ground electronic state, we can state with certainty that the rearrangement occurs in the ground state. As a result of this rearrangement, the C═O group can no longer be thought to possess a group frequency; rather, it becomes strongly vibrationally coupled to the phenyl ring modes. It is likely, as will be discussed below, that strong polarizing forces in the active site bring about the observed electron rearrangement and that valence bond structures resembling the quinone methide structures seen in Figure 2 assume increasing importance. In the simplest sense, we can see that an increase in the contribution from the quinone methide forms will lead to a reduction in the bond order of the C═O bond and lower the force constant into a region where strong mixing with the phenyl modes is expected.

For 4-MeBA-CoA, the Active Site Causes a Strong Localized Polarization of C═O. Further insight into the polarizing forces acting in the active site comes from consideration of the substrate analog 4-methylbenzoate-CoA (4-MeBA-CoA). This binds strongly to dehalogenase (K_i = 4 μM) but does not react. Benzoyl-CoA has a K_i of 70 μM, and the 4-methyl group, which is roughly the same size as a chlorine atom, is thought to be an important contributor to the binding of 4-MeBA-CoA (*6*). A major difference between 4-MeBA-CoA and the product, 4-HBA-CoA, is that

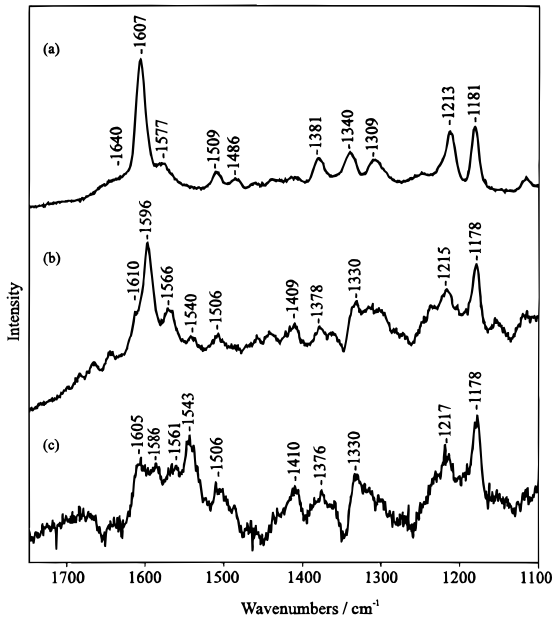

FIGURE 3: Raman difference spectra of (a) C═^{18}O-labeled, unbound, 5 mM 4-MeBA-CoA, (b) 1 mM unlabeled 4-MeBA-CoA bound to 1 mM dehalogenase, and (c) 0.5 mM C═^{18}O-labeled 4-MeBA-CoA bound to 1 mM dehalogenase. All solutions were in 50 mM Hepes at pH 7.5. The spectroscopic conditions were 647.1 nm Kr laser excitation, 750 mW, and 40 accumulations of 10 s each.

the 4-OH group of the latter can assist in polarization in the benzoyl moiety via an intramolecular (resonance) effect while the 4-Me group of the substrate analog cannot.

Raman spectra of unlabeled 4-MeBA-CoA free in solution and bound to the dehalogenase have been discussed in a previous publication (*6*). Unlike the 4-HBA-CoA results, the Raman spectrum of the bound (unlabeled) 4-MeBA-CoA resembles the spectrum of the free form quite closely. Here, we report the effects on the Raman spectra of labeling 4-MeBA-CoA with ^{18}O in the carbonyl group (C═^{18}O).

The Raman spectrum of the C═^{18}O isotopomer of the free ligand in buffer is seen in Figure 3a, and it resembles the spectrum of the unlabeled analog very closely (*6*). The main difference between the spectra of the unlabeled and labeled ligands is that the carbonyl stretch seen clearly at 1651 cm^{-1} in the unlabeled analog (*6*) appears as an unresolved shoulder for the C═^{18}O isotopomer (marked at 1640 cm^{-1} in Figure 3a). In the spectrum of the bound, unlabeled 4-MeBA-CoA (Figure 3b), some of the weak features may be due to protein features that have not subtracted to zero in the difference spectrum due to a change in the protein conformation upon ligand binding. However, the main features of the ligand are clearly apparent, viz. the phenyl modes near 1180, 1215, 1566, and 1596 cm^{-1}. The latter two are some 10 cm^{-1} below the values for the free ligand, and this we ascribe to the effects of the active site polarization forces. The shoulder seen at 1610 cm^{-1} was assigned to the C═O stretching frequency of the bound ligand (*6*). Support for this assignment comes from new results for the C═^{18}O-substituted analog. In Figure 3c, we see that the Raman difference spectrum of the bound C═^{18}O isotopomer retains recognizable phenyl modes near 1180 and 1220 cm^{-1} but gives rise to a complex spectral profile in the 1540−1610 cm^{-1} region. At this time, definitive peak assignments are not possible in this region, but we can give a general description of events leading to the observed spectrum.

For 4-MeBA-CoA, the C═O stretch occurs at 1651 cm^{-1} for the "free", unlabeled ligand in aqueous solution, which, in fact, represents the position for the carbonyl hydrogen bonded to water. Strong polarizing forces in the active site reduce this frequency to the 1610 cm^{-1} region as shown by Figure 3b. When the C═O is substituted by ^{18}O, a further downward movement of the C═O frequency occurs for the bound ligand and vibrational coupling occurs between the carbonyl motions and phenyl ring modes, giving rise to the profile seen in Figure 3c. Taken together, the data are consistent with the appearance of the C═O stretching frequency near 1610 cm^{-1} in the unlabeled bound ligand. While some vibrational coupling may occur even within the unlabeled ligand on the enzyme, we can make a semiquantitative estimate of the shift in the C═O frequency. It is clear that the ~40 cm^{-1} shift for the C═O already hydrogen bonded to water at 1651 cm^{-1} to about 1610 cm^{-1} on the enzyme represents the action of strong polarizing forces acting at or near the C═O in the active site. In the following section, we describe hydrogen bonding studies on a model compound which will be used to estimate the equivalent hydrogen bonding strength enthalpies which give rise to the observed C═O shift on the enzyme.

Model Compound Studies Used to Estimate the Strength of C═O Polarizing Forces in the Active Site: A Relationship between Hydrogen Bonding Strength and $\Delta\nu_{C=O}$. Hydrogen bonding is known to decrease the frequency of carbonyl groups to lower energies, and the stronger the hydrogen bonding, the greater the shift in frequency, $\Delta\nu_{C=O}$ (*22*). A recent FTIR study on the hydrogen bonding between α,β-unsaturated esters and alcohols established an empirical relationship between the enthalpy of hydrogen bonding and $\Delta\nu_{C=O}$ (*21*). This relationship was used to determine the strength of hydrogen bonding between active site donors and the acyl group carbonyl in a series of acyl-enzyme intermediates. A similar approach is used here to estimate the effective hydrogen bonding strength to the C═O of 4-MeBA-CoA in dehalogenase's active site.

For the model compound, 4-methylbenzoyl *S*-ethyl thioester, FTIR spectra were obtained in CCl_4 in the presence of one of the hydrogen bond donors: ethanol, phenol, or 3,5-dichlorophenol. The use of an excess of donor reveals a new carbonyl stretch due to hydrogen bonding with the donor. The model compound alone in CCl_4 gave a carbonyl frequency of 1663 cm^{-1}; when excess ethanol is added, a hydrogen-bonded carbonyl peak at 1650 cm^{-1} is revealed. Excess phenol gave a hydrogen-bonded carbonyl peak at 1643 cm^{-1}, and excess 3,5-dichlorophenol gave a peak at 1637 cm^{-1}.

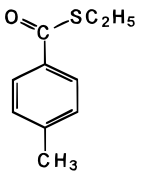

As outlined in Experimental Procedures, FTIR spectra were recorded using various concentrations of model compound with a fixed concentration of donor and *K*, the equilibrium constant was calculated. This was repeated at various temperatures, and the enthalpy of hydrogen bonding was obtained using the van't Hoff equation. The values of $-\Delta H$, ΔS, and $\Delta\nu_{C=O}$ are shown in Table 2.

Table 2: Values of $\Delta\nu_{C=O}$, $-\Delta H$ and ΔS for Each Donor−Model Compound Pair

donor	$\Delta\nu_{C=O}$ (cm^{-1})	$-\Delta H$ (kJ mol^{-1})	ΔS (J K^{-1} mol^{-1})
ethanol	13	7.14	8.96
phenol	20	16.78	40.55
3,5-dichlorophenol	26	23.24	55.42

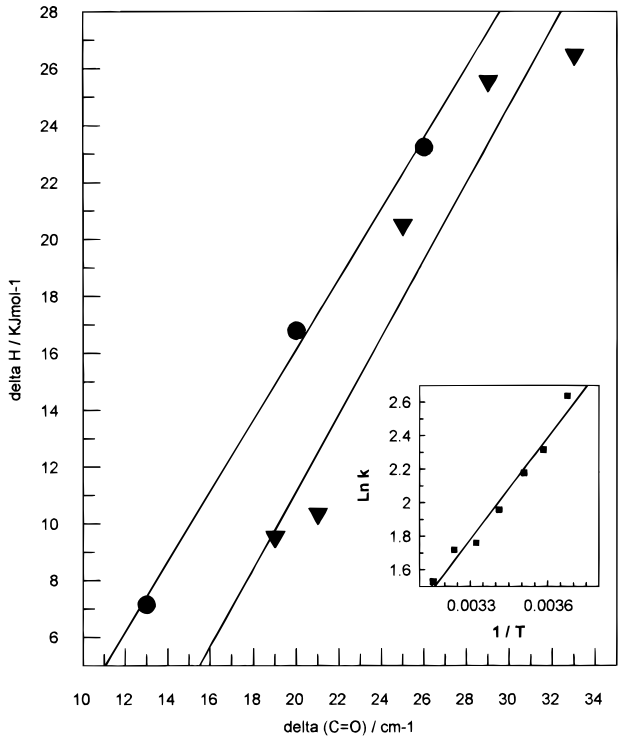

FIGURE 4: Plot of $-\Delta H$ vs $\Delta\nu_{C=O}$ using the data presented in Table 2 for 4-methylbenzoyl *S*-ethyl thioester (data points shown as ●). The data have been fitted by linear regression to the equation $-\Delta H = 1.24\Delta\nu_{C=O} - 8.72$. Data (▼) from a similar study on the α,β-unsaturated esters, 5-methylthienylacryloyl and thienylacryloylmethyl esters are presented for comparison. A van't Hoff plot for phenol and 4-methylbenzoyl ethyl thiolester is shown as an inset.

A plot of $-\Delta H$ against $\Delta\nu_{C=O}$ is shown in Figure 4. The plot fits the equation

$$-\Delta H = 1.24\Delta\nu_{C=O} - 8.72 \qquad (1)$$

Previous data obtained from α,β-unsaturated esters 5-methylthienylacryloyl-OMe and thienylacryloyl-OMe are shown for comparison (*21*), and we can see that the relationships between the carbonyl shifts and enthalpies of hydrogen bonding for the two sets of compounds are very similar. The new data can be used to estimate the change in the "effective hydrogen bonding" observed for 4-MeBA-CoA upon binding to the active site of dehalogenase. The value of $\nu_{C=O}$ for the model compound 4-methylbenzoate *S*-ethyl thioester in CCl_4 is 1663 cm^{-1}, and that for the bound substrate analog is near 1610 cm^{-1}. Thus, $\nu_{C=O}$ shifts by approximately 53 cm^{-1} which, using eq 1, can be ascribed to an equivalent hydrogen bonding strength of 57 kJ mol^{-1}. It is notable that these values are similar in magnitude to the maximal variation in $\nu_{C=O}$ and hydrogen bond strengths reported for a series of acyl serine proteases (*23*). For the latter, a change in hydrogen bonding strength to an active site carbonyl of 57 kJ mol^{-1} corresponded to a change in reactivity of 17000-fold, as expressed by the deacylation rate constants, across the series.

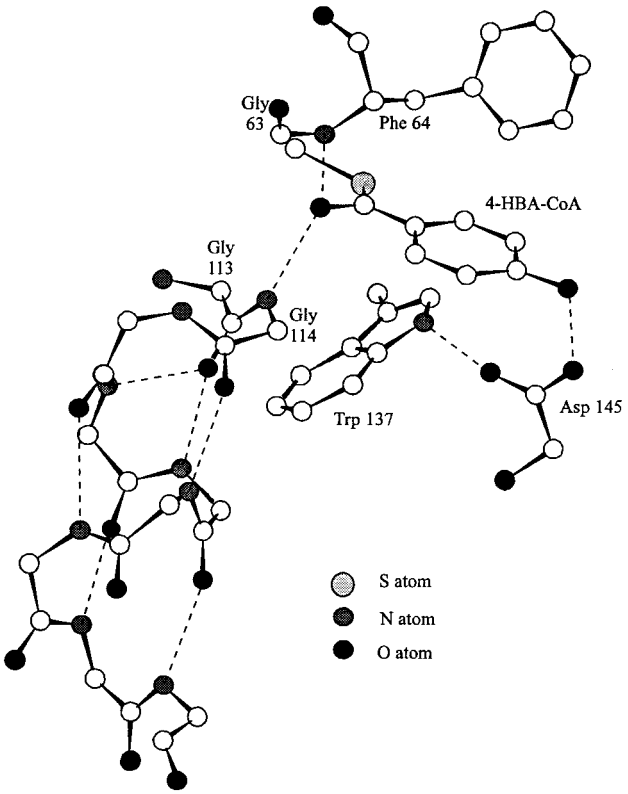

FIGURE 5: Detail from the X-ray structure of 4-HBA-CoA bound to 4-CBA-CoA dehalogenase (*7*), showing interactions at the benzoyl moiety of 4-HBA-CoA.

The Principal Causes of the Large Polarizing Force Are an α-Helix Dipole and Hydrogen Bonds to the Benzoyl Carbonyl. The crystallographic structure of a dehalogenase−4-HBA-CoA complex has been solved recently (*7*) and offers an explanation for the large polarization effects we have described above. Some of the key components are shown in Figure 5. Thus, the peptide amide hydrogens of Phe64 and Gly114 form hydrogen bonds to the carbonyl oxygen of 4-HBA. Moreover, an α-helix formed by residues 121−114 "runs toward" the benzoyl carbonyl with the helix's N terminus (residue 114) approaching the carbonyl group. The propinquity of the helix, with its associated α-helix dipole, provides an electrostatic component to the polarization we have measured.

Examination of the hydrogen bonding network in the vicinity of the N terminus of the α-helix 114−121 reveals how the Gly114 amide hydrogen is positioned to be available for bonding to the thiolester carbonyl of 4-HBA-CoA. The α-helix 114−121 displays the usual $i + 4$ carbonyl to amide hydrogen bonds. However, the N terminus has an α_N distortion, with Gly114 displaying a 3_{10} α-helix turn. This allows the carbonyl of Gly113 to accept hydrogen bonds from the amides of residues Leu116 and also Gly117, $i + 3$ and $i + 4$. These *two* hydrogen bonds to the carbonyl of the peptide bond of Gly113−Gly114 provides extra polarization to the localized dipole of this peptide group, and this dipole is aligned between the $i + 3$ and $i + 4$ dipoles of the α-helix. The conformational freedom that the GlyGlyGly (113−115) tripeptide confers to the N terminus of the helix is likely an important feature for the N terminus cap. In this regard, it has been noted that the phosphate binding α-helix of many dinucleotide binding proteins almost always starts with a glycine and this is a property shared by other "active site helices" (*24*). It has been suggested that the absence of a side chain at the N terminus of these helices allows for a close approach of the substrate.

The alignment of the amide nitrogens of Gly114 and Phe64 is near ideal for hydrogen bonding to the thioester carbonyl of 4-HBA-CoA (Figure 5). However, the hydrogen bond donated by the backbone amide of Phe64 does not display any unusual features, and the carbonyl group of the peptide bond Phe64−Gly 63 is not hydrogen-bonded to any other residue in the protein. The phenyl group of Phe64 is oriented away from the thioester carbonyl of 4-HBA-CoA and contributes to the hydrophobic environment surrounding the benzoyl moiety of 4-HBA-CoA. The Gly63 permits the close approach of the thiolester carbonyl to the amide of Phe64.

In their classic study of hydrogen bonding between molecules of *N*-methyl acetamide, Klotz and Franzen (*25*) showed that the enthalpy of hydrogen bonding between C═O and H−N reaches a maximum of −4.2 kcal mol^{-1} (17.5 kJ mol^{-1}) for the association in CCl_4. This value is reduced as the dielectric constant of the solvent is raised and would almost certainly be significantly less within a protein. Thus, if we make the assumption that the strength of hydrogen bonds from peptide NHs to amide C═Os is approximately the same as that between amide NHs and a thioester C═O, the maximum hydrogen bonding strength we could expect from the two peptide NHs in the active site to the benzoyl C═O is 35 kJ mol^{-1}, with the likelihood that it is considerably less. The additional factor which raises the effective hydrogen bonding strength to the observed 57 kJ mol^{-1} is the electrostatic field associated with the α-helix dipole. The recent consensus is that the electrostatic field arises from localized microscopic dipoles of the peptide residues, with the effect being localized in the first one or two turns of the helix (*9*). Thus, we expect the localized dipoles associated with residues 114−117 to be major contributors to the α-helix dipole-induced polarization in the benzoyl group and its C═O.

The electron pull resulting from the α-helix dipole and the hydrogen bonds to the benzoyl C═O is aided by the hydrophobic environment about the benzoyl ring, which provides a sheath with a low dielectric constant. The benzoyl ring of 4-HBA-CoA is surrounded by Phe64, Trp89, Phe82, Gly114, Trp137, Ile142, and Thr146, all of which lie within 5 Å. Thus, in a sense, the benzoyl moiety is akin to a wire of π-electrons lying within a sheath of insulating material, and this heterogeneous environment provides a means of redistributing charge within the benzoyl π-system and promoting attack by the COO^- side chain at C4.

The X-ray structure also provides a rationale for the different properties observed for bound 4-HBA-CoA and 4-MeBA-CoA. The former shows far greater polarization effects in the active site, a red shift of ∼80 nm compared to a red shift of ∼40 nm for 4-MeBA-CoA (*6*, *8*). The larger red shift is accompanied by a major rearrangement of the vibrational normal modes, whereas only modest changes are seen in the Raman spectrum of 4-MeBA-CoA. Although there is structural data only for the product complex, it is likely that the 4-methyl analog binds in a very similar manner. Thus, the hydrogen bonding and α-helix dipole interactions described above will likely be found in both complexes. The differences in the two complexes reside in the intramolecular electron-releasing propensities of the *para*

substituents. The X-ray structure shows that the only polar residues near the benzoyl ring of 4-HBA-CoA are His90 and Asp145. These are located near the 4-hydroxy position of the benzoyl ring of 4-HBA-CoA with the carboxylate group of Asp145 forming a hydrogen bond with the 4-hydroxy oxygen atom of 4-HBA-CoA. In this situation, the 4-OH and Asp145 COO^- side chain share a single protium. The exact position of the protium cannot be determined, but it can effectively be regarded as spending part of its time "off" the OH group and "on" the COOH. This will result in the electron-donating power of the 4-OH group being increased to some value between the Hammett constant for 4-OH (-0.38) and that for 4-O^- (-0.81) (*26*). Such a situation cannot arise for 4-Me and Asp145, the electron-releasing power of 4-Me, with a Hammett constant of -0.14, prevails. The outcome is that the 4-HBA-CoA ligand has a far greater potential for internal electron release at the *para* position. In valence bond terms, this means that canonical forms akin to the quinone methide forms seen in Figure 2, which bring about major electron polarization, make a large contribution to the true structure. Whereas the equivalent form for 4-MeBA-CoA does not exist, and therefore, electron rearrangement and polarization are less pronounced. A further effect which could reduce polarization in the bound 4-MeBA-CoA moiety is repulsion between the 4-Me group and the side chain of Asp145 which could reduce interactions between the product's phenyl ring and active site aromatic side chains. In turn, this would reduce the "insulating" effect of the aromatic sheath.

REFERENCES

1. Dunaway-Mariano, D., and Babbitt, P. C. (1994) *Biodegradation 5*, 259.
2. Yang, G., Liang, P. H., and Dunaway-Mariano, D. (1994) *Biochemistry 33*, 8527.
3. Liu, R., Liang, P. H., Scholten, J., and Dunaway-Mariano, D. (1995) *J. Am. Chem. Soc. 117*, 5003.
4. Bernasconi, C. F. (1980) *Chimia 34*, 1.
5. Miller, J. (1968) in *Reaction Mechanisms in Organic Chemistry* (Eaborn, C., and Chapman, N. B., Eds.) Monograph 8, Elsevier, New York.
6. Taylor, K. L., Liu, R., Liang, P. H., Price, J., Dunaway-Mariano, D., Tonge, P. J., Clarkson, J., and Carey, P. R. (1995) *Biochemistry 34*, 13881.
7. Benning, M. M., Taylor, K. L., Liu, R., Yang, G., Xiang, H., Wesenberg, G., Dunaway-Mariano, D., and Holden, H. M. (1996) *Biochemistry 35*, 8103.
8. Taylor, K. L., Xiang, H., Liu, R.-Q., Yang, G., and Dunaway-Mariano, D. (1997) *Biochemistry 36*, 1349.
9. He, J. J., and Quiocho, F. A. (1993) *Protein Sci. 2*, 1643.
10. Kortemme, T., and Creighton, T. E. (1995) *J. Mol. Biol. 253*, 799.
11. Sali, D., Bycroft, M., and Fersht, A. R. (1988) *Nature 335*, 740.
12. Carey, P. R., and Storer, A. C. (1984) *Annu. Rev. Biophys. Bioeng. 13*, 25.
13. Lockhart, D. J., and Kim, P. S. (1992) *Science 257*, 947.
14. Hol, W. G., van Duijjnen, P. T., and Berendsen, H. J. C. (1978) *Nature 273*, 443.
15. Doran, J. D., and Carey, P. R. (1996) *Biochemistry 35*, 12495.
16. Doran, J. D., Tonge, P. J., Mort, J. S., and Carey, P. R. (1996) *Biochemistry 35*, 12487.
17. Chang, K. H., Liang, P. H., Beck, W., Scholten, J. D., and Dunaway-Mariano, D. (1992) *Biochemistry 31*, 5605.
18. Liang, P. H., Yang, G., and Dunaway-Mariano, D. (1993) *Biochemistry 32*, 12245.
19. Merkel, S. M., Eberhard, A. E., Gibson, J., and Harwood, C. S. (1989) *J. Bacteriol. 171*, 1.
20. Kim, M., Owen, H., and Carey, P. R. (1993) *Appl. Spectrosc. 47*, 1780.
21. Tonge, P. J., Fausto, R., and Carey, P. R. (1996) *J. Mol. Struct. 379*, 135.
22. Pimentel, G. C., and McClellan, A. L. (1960) in *The Hydrogen Bond*, W. H. Freeman, San Francisco.
23. Carey, P. R., and Tonge, P. J. (1995) *Acc. Chem. Res. 28*, 8.
24. Wierenga, R. K., De Maeyer, M. C. H., and Hol, W. G. (1985) *Biochemistry 24*, 1346.
25. Klotz, I. M., and Franzen, J. S. (1962) *J. Am. Chem. Soc. 84*, 3461.
26. March, J. (1992) in *Advanced Organic Chemistry*, Wiley Interscience, New York.
27. Varasanyi, G. (1969) in *Vibrational Spectra of Benzene Derivatives*, Academic Press, New York.

BI970941X